Water Resources Research

DATA ARTICLE
10.1029/2022WR033006

A Meteorology and Snow Data Set From Adjacent Forested and Meadow Sites at Crested Butte, CO, USA

Hannah M. Bonner[1], Eric Smyth[1], Mark S. Raleigh[2], and Eric E. Small[1]

[1]Department of Geological Sciences, University of Colorado, Boulder, CO, USA, [2]College of Earth, Ocean, and Atmospheric Sciences, Oregon State University, Corvallis, OR, USA

Key Points:

- We describe a detailed, multiyear snowpack and meteorological data set collected in a paired forest-open setting in a continental climate
- Meteorological observations are processed for quality and continuity and supplemented with downscaled and assimilated precipitation
- The data set can support snow model evaluations and ongoing community investigations on snow-forest processes and mountain hydrometeorology

Supporting Information:

Supporting Information may be found in the online version of this article.

Correspondence to:

H. M. Bonner and M. S. Raleigh,
hannah.bonner@colorado.edu;
raleigma@oregonstate.edu

Citation:

Bonner, H. M., Smyth, E., Raleigh, M. S., & Small, E. E. (2022). A meteorology and snow data set from adjacent forested and meadow sites at Crested Butte, CO, USA. *Water Resources Research*, *58*, e2022WR033006. https://doi.org/10.1029/2022WR033006

Received 9 JUN 2022
Accepted 1 SEP 2022

Abstract We present meteorology and snow observation data collected at sites in the southwestern Colorado Rocky Mountains (USA) over three consecutive water years with different amounts of snow water equivalent (SWE) accumulation: A year with above average SWE (2019), a year with average SWE (2020), and a year with below average SWE (2021). This data set is distinguished by its emphasis on paired open-forest sites in a continental snow climate. Approximately once a month during February–May, we collected data from 15 to 20 snow pits and took 8 to 19 snow depth transects. Our sampling sites were in open and adjacent forested areas at 3,100 m and in a lower elevation aspen (3,035 m) and higher elevation conifer stand (3,395 m). In total, we recorded 270 individual snow pit density and temperature profiles and over 4,000 snow depth measurements. These data are complimented by continuous meteorological measurements from two weather stations: One in the open and one in the adjacent forest. Meteorology data—including incoming shortwave and longwave radiation, outgoing shortwave radiation, relative humidity, wind speed, snow depth, and air and infrared surface temperature—were quality controlled and the forcing data were gap-filled. These data are available to download from Bonner, Smyth, et al. (2022) at https://doi.org/10.5281/zenodo.6618553, at three levels of processing, including a level with downscaled, adjusted precipitation based on data assimilation using observed snow depth and a process-based snow model. We demonstrate the utility of these data with a modeling experiment that explores open-forest differences and identifies opportunities for improvements in model representation.

1. Introduction

Understanding snow-forest interactions is critical for characterizing and predicting snowpack, across basins and at sites worldwide (Rutter et al., 2009). Field observations are essential for improving our process knowledge and for assessing model predictions of snow water equivalent (SWE) and other states (Essery et al., 2009; Lundquist et al., 2021; Mazzotti, Essery, Webster, et al., 2020; Moeser et al., 2016; Rutter et al., 2009; Strasser et al., 2011). Model improvements can be facilitated by data collected in the field, including measuring the interception and unloading of canopy snow (e.g., Hedstrom & Pomeroy, 1998; Raleigh et al., 2022; Storck et al., 2002) and observing the forest-altered energy balance regime (e.g., Malle et al., 2019; Musselman & Pomeroy, 2017). Ongoing improvement and validation of SWE predictions and snow models require detailed field observations of forest-snow processes (Bonner, Raleigh, & Small, 2022).

Only a subset of snow data sets facilitate studies of forest-snow processes. Operational data sets (e.g., NRCS SNOTEL) use automated observations (sonic snow depths and snow pillows) in forest clearings that do not characterize the heterogeneous snowpack in the surrounding forest. Other snow research sites provide multiple manual measurements (snow pits) in open environments but lack replicate data collection in adjacent forests (e.g., Landry et al., 2014; Lejeune et al., 2019; Wayand et al., 2015). In recent years, some snow data sets have included observations from paired open-forest sites (e.g., Fang et al., 2019; Reba et al., 2011; Roth & Nolin, 2017; Teich et al., 2019), which enable investigations of the impact of forest effects on snowpack in various types of climates. The data presented in this publication add to this latter body of work and provide forest and open snow observations for a continental snow climate.

The field observations presented here were collected across three water years (WY, 1 October–30 September) 2019–2021. This data set is distinguished by its extensive snow pit and snow transect data collected in paired forested and open environments, each with identical meteorological data collection. The data set uniquely emphasizes the utility of continuous meteorological and detailed snow pit and transect data for quantifying forest effects

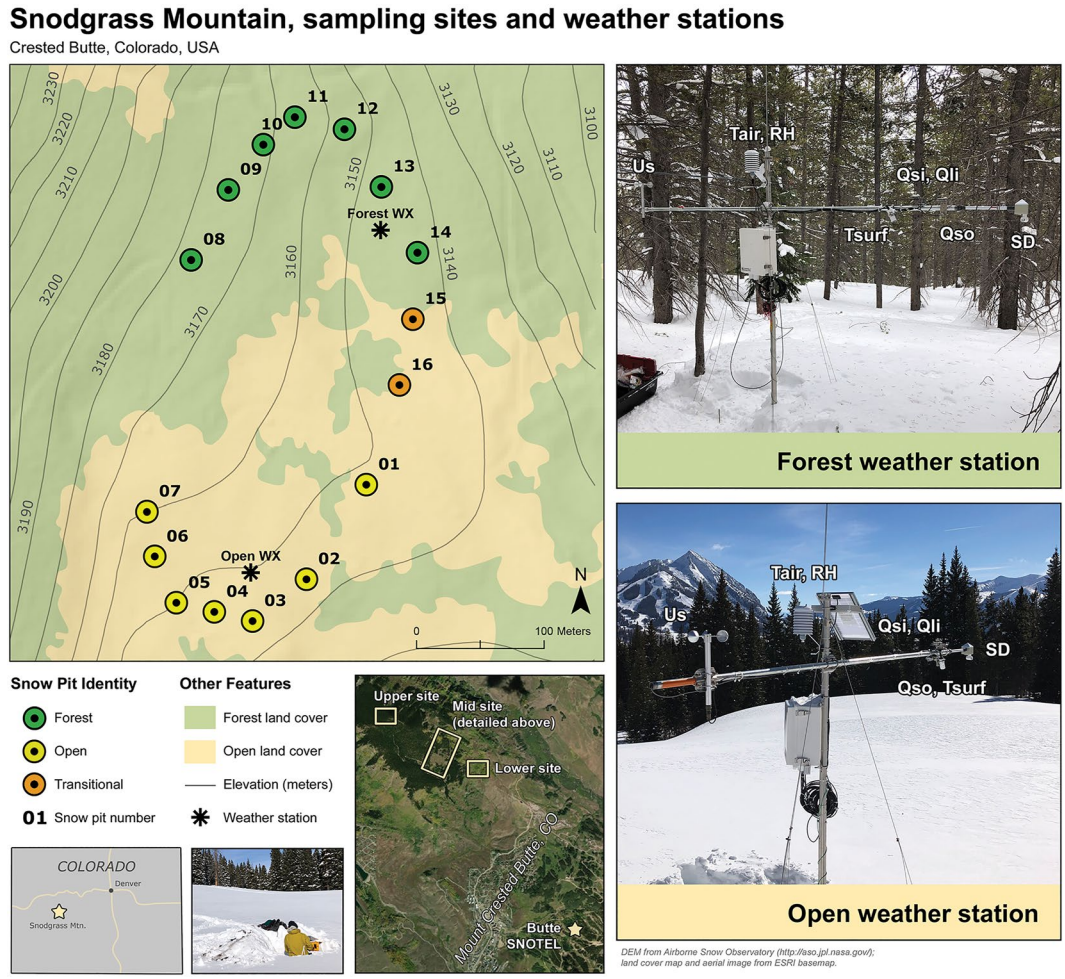

Figure 1. Snodgrass Mountain field site. The snow pit layout in the top left map was the design for WY 2019 (see text). Snow transects were taken in a ~50 × 50 m square centered around each pit location. Variables measured at the weather stations (right photos) are as follows: Air temperature (T_{air}), relative humidity (RH), wind speed (Us), incoming shortwave radiation (Q_{si}), incoming longwave radiation (Q_{li}), outgoing shortwave radiation (Q_{so}), IR surface temperature (T_{surf}), and snow depth (SD).

on snowpack characteristics, expanding understanding of snow-forest interactions, and improving model predictions of SWE, surface energy balance, and climate.

2. Study Site

The data were collected on Snodgrass Mountain (38°55'38"N, 106°58'46"W), located near Crested Butte, Colorado, USA, in the southwestern Rocky Mountains (Figure 1). Snodgrass Mountain is situated in the East River Basin, a tributary to the Colorado River. Several scientific campaigns have converged in the East River Basin, including work by NASA (SnowEx; Elder et al., 2018), the U.S. Department of Energy, NOAA (i.e., SPLASH), and long-term environmental measurements by the nearby Rocky Mountain Biological Laboratory (Gothic, CO). The Butte (site 380) snowpack telemetry (SNOTEL) station is located ~4 km to the southeast.

Snodgrass Mountain is largely forest covered from 2900 m elevation to the summit at 3,400 m (Figure 1). Forests are dominated by subalpine conifers, commonly Engelmann spruce (*Picea engelmannii*) and subalpine fir (*Abies lasiocarpa*), with occasional stands of quaking aspen (*Populus tremuloides*; Crawford et al., 1998). Typical tree height in the study area is 9 m with a leaf area index (LAI) of 4. Additional canopy data are available from the Colorado East River Community Observatory (Kakalia et al., 2021). The area exhibits a continental snow climate, characterized by dry, cold air and frequent winter snow storms (Trujillo & Molotch, 2014). Over a 30-year period (1991–2021), the Butte SNOTEL has an average peak SWE of 390 mm, average annual temperature of 2.8°C, and average winter

(December–February) temperature of −6.7°C. The three water years examined differed in peak SWE: WY 2019 was above average (493 mm); WY 2020 was near average (345 mm); WY 2021 was below average (282 mm).

Manual snow surveys were conducted on Snodgrass Mountain at multiple locations. The primary study site and weather stations were located at approximately 3,100 m elevation on flat ground (or local slopes less than 5°) at paired open (meadow) and forest (subalpine conifer) environments. In WY 2019, 16 sites within a 0.5 km distance were used: Seven sites in the open (sites 1–7; Figure 1), seven sites in the forest (sites 8–14), and two sites in an open-forest transitional zone (sites 15–16). To increase data collection efficiency, sites were consolidated in WY 2020 and 2021 to three open sites (sites 2, 4, and 6) and three forest sites (sites 12–14). Two weather stations were installed within this array of field sites: One in the open (38°55'35.7"N, 106°58'44.1"W) and one in the forest (38°55'44.5"N, 106°58'40.1"W), at a horizontal separation of 300 m (Figure 1). Snow surveys were also conducted at two additional forested sites to examine elevation effects on snowpack: A lower elevation aspen stand (~3,035 m) and an upper elevation conifer forest at the summit (~3,395 m; Figure 1).

3. Snow Data

3.1. Snow Pit Data

We collected snowpack measurements approximately once a month, typically during February–May. At each visit to the primary, midmountain study site, we dug 7–9 snow pits in both forested and open locations, totaling 14–18 pits (Table S1 in Supporting Information S1). Additionally, 1–3 snow pits each were dug at both the lower and upper elevation sites. In total, 84–95 snow pits were dug and recorded each water year, totaling 270 snow pits over the initial three-year period.

Snow pit measurements were focused on snow depth and vertical profiles of snow density and temperature. Snow depth was measured directly in each pit using a ruler; snow density was measured in 10 cm increments using a 1000-cc snow cutter; and snowpack temperature was measured every 10 cm using a digital thermometer (Figure S1, Text S1 in Supporting Information S1). Observed depth and bulk density were used to calculate SWE. All digitized snow pit observations were combined into a single summary file that included pit location, site type, snow depth, average snow density, bulk SWE, average temperature, and cold content (Figure S2, Text S1, and S2 in Supporting Information S1). Pit-specific files, including the full profile data, are also included in the dataset (Bonner, Smyth, et al., 2022).

At the midmountain, primary study site, snowpack density profiles varied with year, season, and between forest and open sites (Figure 2). Here, we present profiles generated by calculating the average density of all open ($n = 96$) or forest ($n = 154$) snow pits within a set 10 cm depth window. Snow pits with total depth that differed by more than ±20 cm from the median open or forest snow pit depth were excluded. Open sites generally had greater overall density than forest sites, but both open and forest sites followed a similar vertical pattern of density. During the accumulation season (Figures 2a and 2b), snow density tended to be highest at one third of the maximum snow depth and lowest at the snow surface. Snow density profiles became more uniform once ablation began, especially at the open sites (Figure 2c, Table S2 in Supporting Information S1). Higher density at the snow surface was common in the late melt season (Figure 2d). Depth, density, and SWE were generally higher at the higher elevation sites (Table S2 in Supporting Information S1).

3.2. Snow Depth Transects

Snow depth measurements were taken along the perimeter of a ~50 × 50 m square centered around each snow pit, with six depth measurements on each side (24 total). Either eight (WY 2020 and 2021) or 19 (WY 2019) transects were collected per visit, totaling 154 transects (over 4,000 individual depth measurements) during the three-year sampling period (Table S1 in Supporting Information S1). The average depth in transects was very similar to corresponding snow pits, indicating snow pit data were collected in representative locations (Figure S3, Text S3 in Supporting Information S1). Likewise, snow depth coefficient of variation was generally <10% until the melt season (Table S2 in Supporting Information S1).

4. Meteorological Data

Meteorological data collection began at the weather stations in water year 2019 and is ongoing. Both stations were equipped with an identical array of sensors that measured air temperature (naturally ventilated), relative

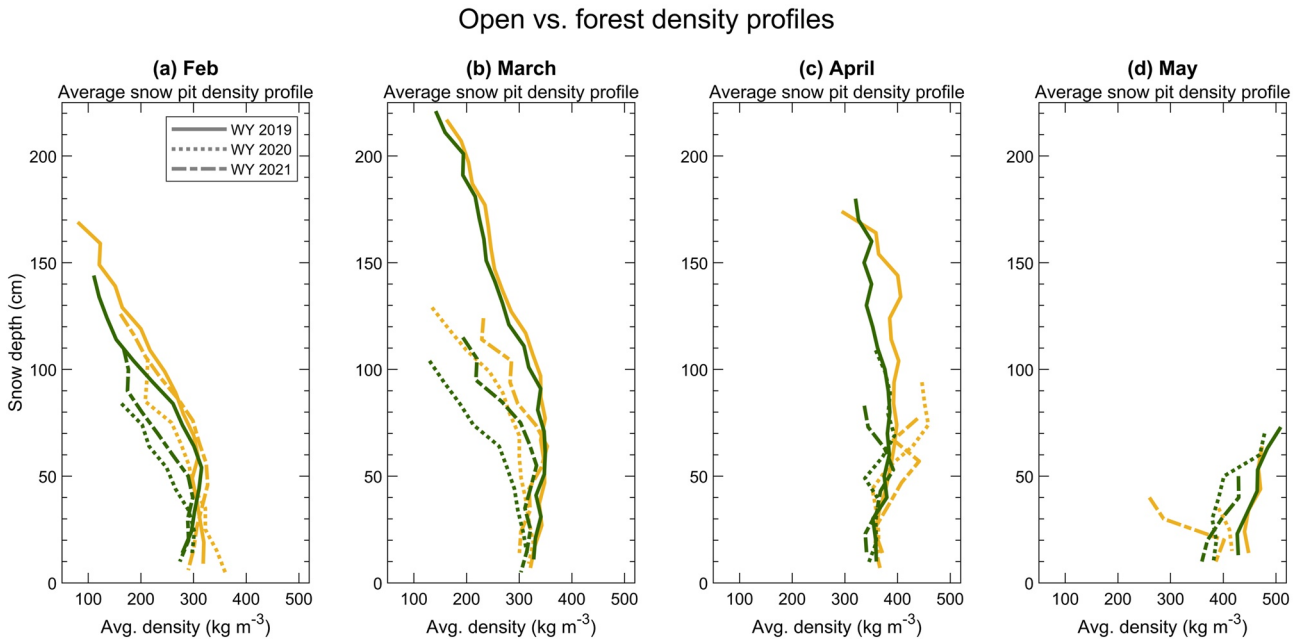

Figure 2. Average snow pit density profiles at the midmountain sites during monthly visits during WY 2019–2021. Yellow lines represent open sites, green lines represent forest sites.

humidity, wind speed, snow depth, incoming and reflected shortwave radiation, incoming longwave radiation, and infrared (IR) surface temperature (Table 1, Figure 1). Both uplooking radiometers had heaters to reduce snow capping. From these data, outgoing longwave radiation, daily albedo, and dew point temperature were calculated.

4.1. Precipitation Data and Adjustments

A precipitation gauge was not deployed in the initial study period, as snowfall measurements are vulnerable to undercatch errors of 20%–50% (Kochendorfer et al., 2017; Rasmussen et al., 2012). Instead, we produced our best estimate of hourly precipitation based on downscaling and assimilation of hourly North American Land Data Assimilation System (NLDAS-2) reanalysis data at a 1/8° spatial resolution. We used MeteoIO to downscale precipitation using the inverse distance weighting with elevation detrending/reprojection (IDW_LAPSE) technique (Bavay & Egger, 2014).

Downscaled precipitation data were then further adjusted via data assimilation to ensure that estimated snowfall rates corresponded to the observed snowpack evolution at the stations. We assimilated each station's daily snow depth measurements into a snow model (Flexible Snow Model, FSM2, Essery, 2015) using a Particle Filter (PF) assimilation method. The PF is an ensemble-based method to generate best estimates of states and fluxes (e.g., hourly precipitation) through time, while accounting for both model and observational uncertainties. Individual model runs, or particles, are forced with observed meteorological data that is perturbed to reflect stochastic and systematic measurement errors. Those particles are then weighted based on their agreement with observations (here, daily snow depth). In this way, the PF identifies particles with perturbations (e.g., to precipitation) that generate the most accurate snowpack estimates—thus generating site-specific open and forest precipitation data. We generated ensembles of particles by perturbing the model forcing inputs and by varying a sensitive snow compaction parameter. The full PF assimilation methodology is described in Smyth et al. (2020).

FSM2 does not partition rain and snow, so we preprocessed the downscaled precipitation using a dew point temperature threshold of 0°C. In the model, the density of freshly fallen snow is adjusted from a default value of 100 kg m^{-3} based on concurrent wind speed and air temperature, using the methodology of the Crocus snow model (Brun et al., 1989).

At the forest station, observed snow depth is not only a function of precipitation—it is influenced by the forest canopy: Interception losses and subsequent unloading of snowfall, shading of shortwave radiation, and increased down-

Table 1
Sensors Deployed at Open and Forest Site Weather Stations and Quality Control Values (See Section 4.2.1)

Measurement	Variable name(s)	Sensor (supplier)	Specified sensor accuracy	Sensor height (m; open site)	Sensor height (m; forest site)	Quality control values: Min. value	Max. value	Max. rate of change (h^{-1})	Max. time steps with no change (h)
Air temperature	T_{air}	EE-181 (Campbell Scientific)	±0.2°C	2.8	2.2	−40°C	40°C	15°C	4
Relative humidity	RH	EE-181 (Campbell Scientific)	±(1.5 + 0.015 *x* RH)%	2.8	2.2	5%	100%	50%	4
Wind speed	Us, Us_max	014A (Met One)	±0.11 m s^{-1}	3.2	2.9	0 m s^{-1}	50 m s^{-1}	--	5
Incoming shortwave radiation	Q_{si}	SP-510 Thermopile Pyranometer (Apogee)	<3%	3.2	2.8	0 W m^{-2}	1360 W m^{-2}	1000 W m^{-2}	16
Reflected shortwave radiation	Q_{so}	SP-610 Thermopile Pyranometer (Apogee)	<3%	3.2	2.8	0 W m^{-2}	1360 W m^{-2}	1000 W m^{-2}	16
Incoming longwave radiation	Q_{li}	SL-510 Thermopile Pyrgeometer (Apogee)	±5%	3.2	2.8	80 W m^{-2}	440 W m^{-2}	350 W m^{-2}	3
IR surface temperature	T_{surf}	SI-121 Infrared Radiometer (Apogee)	±0.2°C	2.9	2.6	−40°C	40°C	15°C	4
Snow depth	SD	Ultrasonic Depth Sensor (Judd)	±1 cm	3.1	2.7	0 cm	250 cm	10 cm	70

welling longwave radiation (Conway et al., 2018; Lundquist et al., 2013; Musselman & Pomeroy, 2017; Musselman et al., 2008, 2015; Varhola et al., 2010). By assimilating these subcanopy snow depth observations with the PF, we implicitly account for these canopy-related processes, generating a time series of effective "subcanopy precipitation" (e.g., Smyth et al., 2020) that accounts for canopy interception losses and corresponds to the observed forest snowpack.

At the open site, WY accumulated precipitation from downscaling and data assimilation was 20%–33% higher than from the nearby SNOTEL, 20%–37% higher than from nondownscaled NLDAS-2, and 0%–13% higher than downscaled only NLDAS-2 data (Figure 3). SWE from snow pits provided a minimum estimate of accumulated precipitation, given some water was lost to sublimation or melt and drainage. The downscaled and assimilated precipitation data were typically closest to snow pit observations, while the unadjusted precipitation data sets fell below the SWE-based minimum estimate (Figure 3). Both downscaled NLDAS-2 precipitation (open weather station) and downscaled and data assimilated precipitation (open and forest weather stations) are included in the dataset.

4.2. Quality Control and Gap-Filling Processes

Three levels of weather station data processing were provided in the data set for both the open and forest sites: Level 1 (L1) are raw data either in 1 min or 5 min time step format; Level 2 (L2) are quality controlled data in an hourly time step format; and Level 3 (L3) are quality controlled and gap-filled data in an hourly time step format (Bonner, Smyth, et al., 2022), a ready-to-use forcing data set for modeling applications.

4.2.1. Quality Control

L2 and L3 weather station data were quality controlled both as raw data and following aggregation into hourly time steps. Following Meek and Hatfield (1994), data were flagged at each time step when one or more of the following occurred: (a) Value was missing; (b) value was outside high/low range limits; (c) value exceeded rate of change limits (hourly data only); and (d) value remained constant longer than a chosen time limit (hourly data only; Table 1). Additionally, shortwave and longwave values were flagged when snow was detected on the radiometer domes (i.e., reflected shortwave exceeded incoming shortwave during daytime, or incoming longwave exceeding 300 W m^{-2} during night with air temperature less than 0°C). This resulted in intermittent gaps in longwave and shortwave radiation data at both the open site (<10% overall; Figure S4 in Supporting Information S1) and the forest site (<20% overall, not considering a 120-day power failure; Figure S5, Table S3 in Supporting Information S1). Flagged values were removed from the L2 data set.

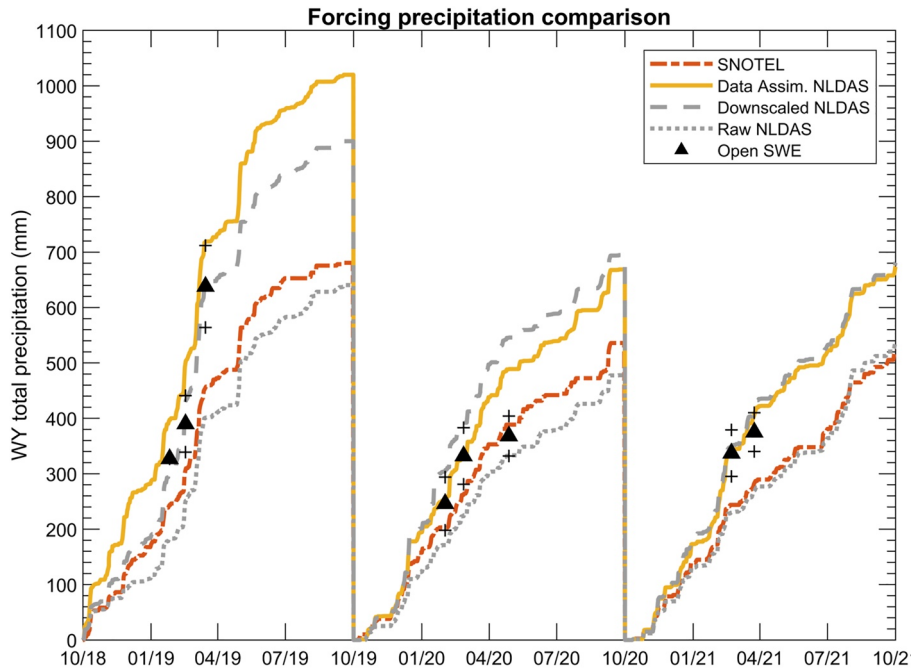

Figure 3. Water year accumulated precipitation at the midmountain open weather station using Butte snowpack telemetry (SNOTEL), nondownscaled North American Land Data Assimilation System (NLDAS-2), downscaled NLDAS-2, and downscaled/assimilated NLDAS-2 data. Median open snow water equivalent (SWE) measured at snow pits is a minimum estimate of accumulated precipitation with interquartile ranges indicated by "+".

4.2.2. Gap-Filling

L3 weather station data were gap-filled to create a continuous hourly forcing data set consisting of air temperature, relative humidity, incoming shortwave, incoming longwave, wind speed, and downscaled and adjusted precipitation. Data were generally complete throughout the monitoring period with less than 25% of the data set gap-filled (Figures S4 and S5 in Supporting Information S1). Shortwave and longwave radiation at the forest site required more extensive gap-filling (40%–45%; Table S3 in Supporting Information S1). Hourly model validation data (e.g., outgoing shortwave, snow surface temperature, and snow depth) were not gap-filled.

Three gap-filling methods were utilized, depending upon the availability of data from the other weather station, length of the gap, and variable. The first was based on station to station relationships. For relative humidity and air temperature, this was a direct replacement due to their high similarity (Figure 4); for incoming shortwave and longwave radiation, this was done using linear regression; for wind speed, this was done using quantile matching similar to other studies (Landry et al., 2014; Ménard et al., 2019; Wayand et al., 2015). Second, we considered mean values from the 24 hr before and after at the same weather station, similar to the method used by Liston and Elder (2006), an effective approach to fill short, sporadic data gaps (e.g., Henn et al., 2013). The third gap-filling method was based on downscaled and bias-corrected NLDAS-2 data. All NLDAS-2 data were downscaled using MeteoIO (Bavay & Egger, 2014). NLDAS-2 data for incoming shortwave and longwave radiation were bias-corrected using linear regression; data for wind speed were corrected using quantile matching; no bias correction was necessary for the downscaled temperature and humidity.

We identified the hierarchy of candidate gap-filling approaches using cross-validation (see Text S4 in Supporting Information S1). We then applied these techniques sequentially until all missing data were gap-filled. Station-to-station gap-filling was the most effective technique in the majority of cases considered.

4.3. Meteorological Data Characterization

Forest canopy effects were observed in the meteorological data (Figure 4). At midday, the open weather station received 450–750 W m^{-2} more incoming shortwave and 65–100 W m^{-2} less incoming longwave than the forest weather station. These differences led to hourly net radiation being 70–80 W m^{-2} higher in the forest at night, but overall daily average net radiation was 31–156 W m^{-2} higher in the open. Despite these differences, air

10.1029/2022WR033006

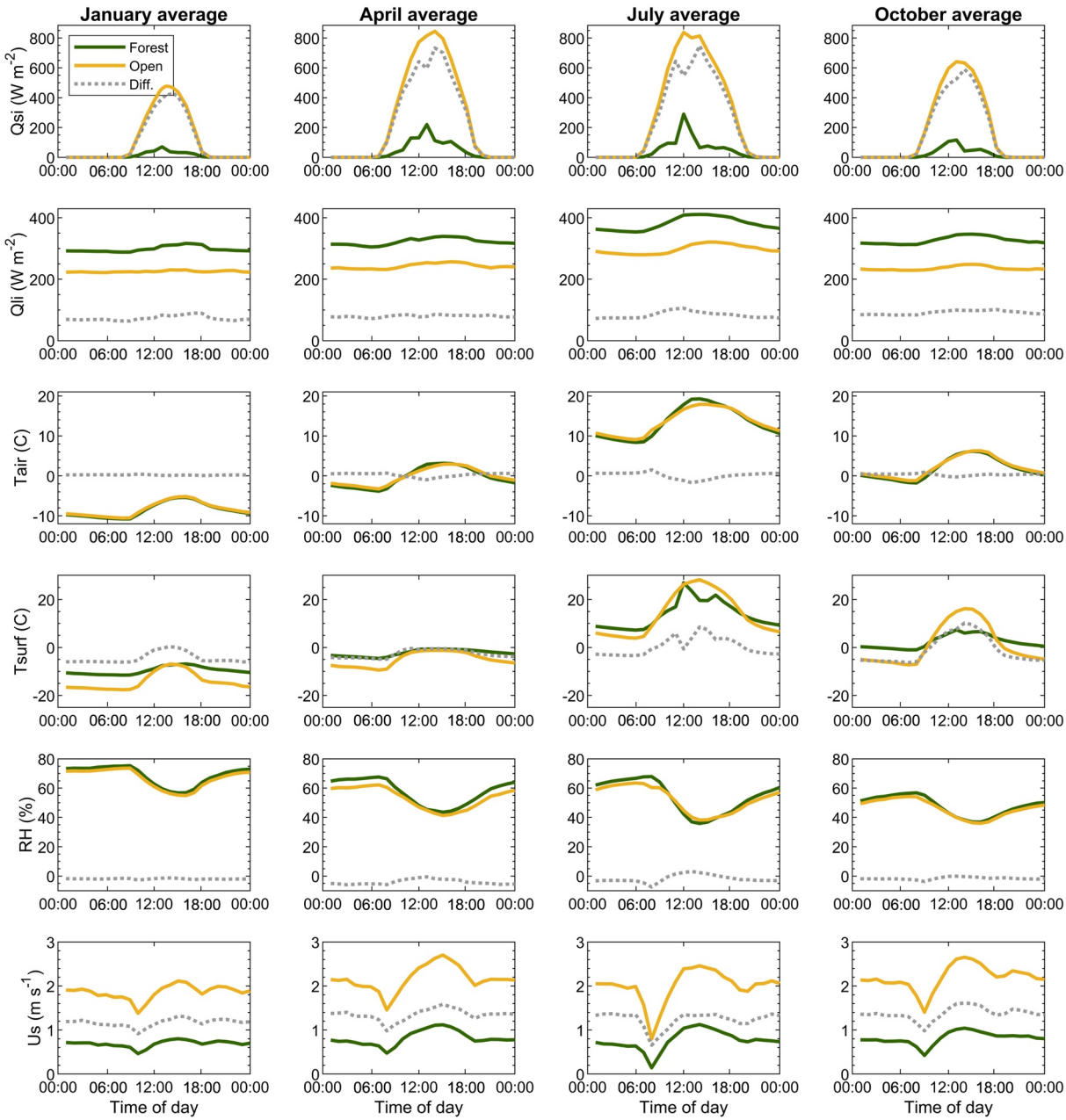

Figure 4. Hourly averages per month as recorded by the forest and open weather stations. The difference between averages in open and forest is also indicated.

temperature remained similar between open and forested sites. However, the snow or ground surface temperature was typically warmer in the forest at night time. Wind speed was typically higher (i.e., >1 m s^{-1}) in the open.

5. Example Application

We conducted a modeling experiment to highlight the utility of this data set for characterizing open-forest snowpack differences and model evaluation. The Factorial Snow Model (FSM2; Essery, 2015; Mazzotti, Essery, Moeser, & Jonas, 2020) was used to simulate snowpack during WY 2019–2021 at the open and forest stations, which are surrounded by the midmountain snow pit and transect sampling sites (Figure 1). FSM2 runs were forced using the respective L3 weather station data with a single configuration and a maximum of 15 layers. No forest canopy was specified at the open site. Because the forest weather station data represent undercanopy

meteorological conditions, we ran FSM2 without a modeled canopy at the forest site. Given this configuration, the precipitation input at the forest site represented the addition of mass to the snowpack after accounting for throughfall, unloading, and canopy losses (e.g., "effective subcanopy precipitation"). We could have used the open weather station data for both sites and ran FSM2 with a modeled canopy for the forest site but we instead chose this approach to utilize all meteorological data. Even though the L3 precipitation data were adjusted using assimilation of site-specific weather station snow depth (see Section 4), the snow pit and snow transect data provide independent checks on model performance.

At the open site, FSM2 matched SWE observations within 40 kg m^{-2}, most bulk density observations within 30 kg m^{-3}, and most depth observations within 20 cm (Figure 5). At the forest site, FSM2 bulk density was similarly close to observations. However, modeled forest SWE was less accurate, especially at and after peak SWE in WY 2019. This resulted from differences in observed and modeled snow depth. FSM2-predicted snow depth was 40–50 cm less than measured in snow pits in March and April 2019. The model underprediction (~30%)

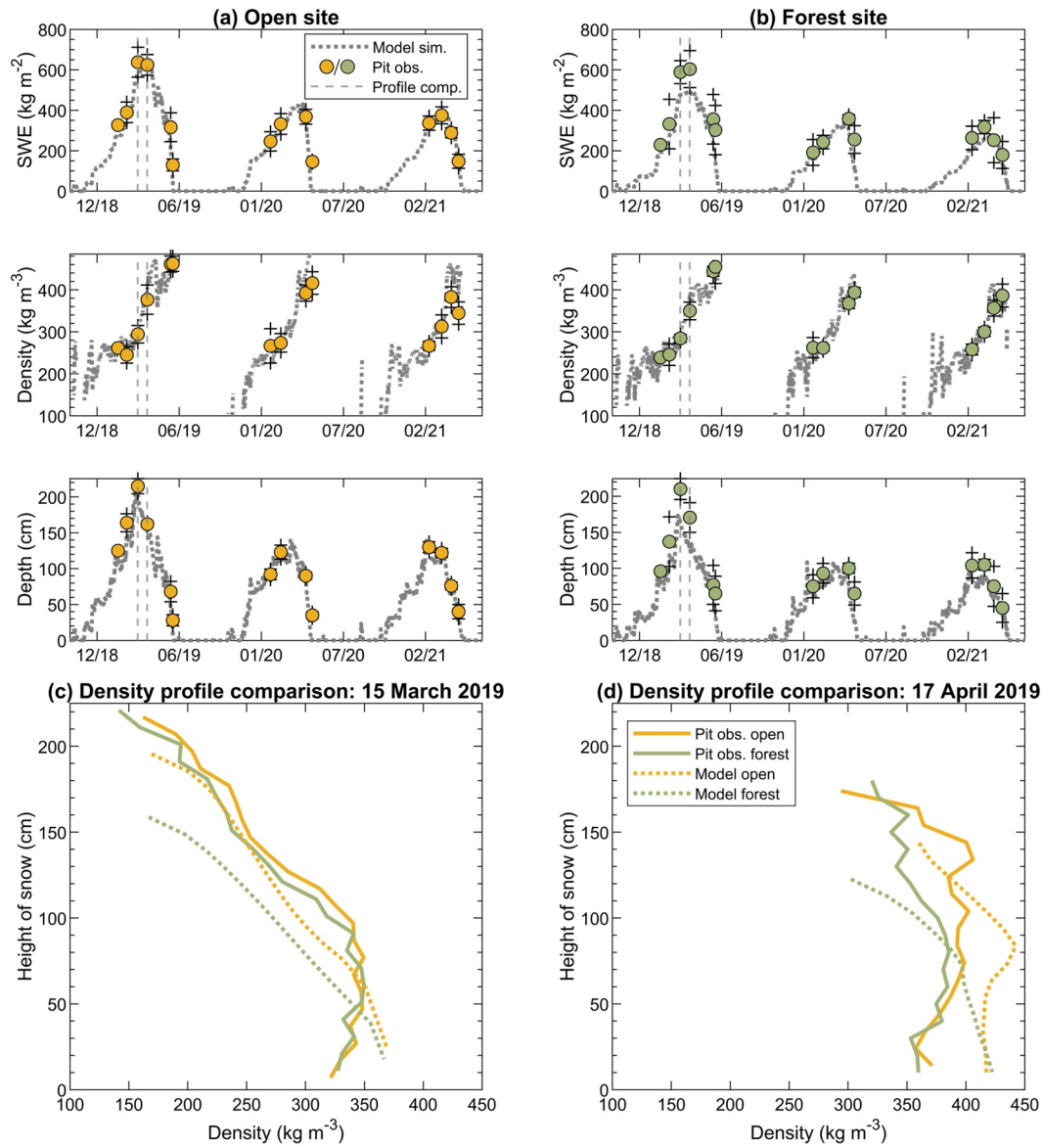

Figure 5. Snow water equivalent (SWE), snow density, and snow depth from FSM2 simulations and snow pit observations. Bulk values (a–b), with interquartile range for snow pit observations (indicated by +), and sampling date specific profiles (c–d) are shown.

was approximately quadruple the coefficient of variability in midmountain forest snow depth (8%; Table S2 in Supporting Information S1). As weather station snow depth was used to adjust the precipitation via data assimilation, this indicated snow depth at the forest weather station was not the same as median forest snow pit depth in WY 2019. However, it was similar in WY 2020 and 2021. This result, particularly in contrast to the consistently accurate performance of FSM2 for the open site, highlights the challenge of representing a heterogeneous forest snowpack and the importance of multiple depth measurements.

The snow pit data were also useful to highlight discrepancies between modeled and observed vertical profiles of snowpack characteristics that were not apparent when considering bulk values. While FSM2 and measured bulk density were similar in March and April of WY 2019 (Figure 5), the snowpack profiles differed considerably (up to 80 kg m^{-3}). The model-predicted snow density was too high near the ground and too low near the snow surface in March 2019. Comparing snowpack profiles is challenging due to difference in simulated and observed depth (e.g., Lehning et al., 2001) but their relative patterns are still instructive. Many snowpack models, including FSM2, do not represent vapor transport due to temperature gradients (Domine et al., 2019). This precludes the development of lower density layers of faceted grains at the base of the modeled snowpack, which can be seen in the March and April 2019 profiles (Figures 5c and 5d). This result demonstrates the utility of this dataset, as a diversity of research questions—ranging from SWE retrievals using remote sensing to investigating the effect of snow layer hardness on animal mobility—relies on accurate modeled snowpack profiles (e.g., Sivy et al., 2018; Venäläinen et al., 2021).

6. Conclusions

Meteorological and snowpack data were collected in a paired open-forest setting near Crested Butte, Colorado. Meteorological measurements from matched forest and open weather stations were quality controlled and gap-filled to provide continuous forcing data for WY 2019–2021. Extensive snow pit (~90 pits per year) and snow transect (~1,300 points per year) data were collected near the weather stations and at higher and lower elevations. These unique data have been made available to the community to support investigations of snow processes and model development in a forested mountain landscape in a continental climate. They also have potential utility to support recent and ongoing campaigns near Crested Butte related to snow remote sensing (NASA SnowEx), land-atmosphere interactions and mountain hydrology (e.g., DOE SAIL), and mountain weather (e.g., NOAA SPLASH). Data collection is ongoing, and the datasets will be expanded annually as new observations are collected and processed.

Data Availability Statement

The datasets described here are available for download from Bonner, Smyth, et al. (2022) at https://doi.org/10.5281/zenodo.6618553.

Acknowledgments
This work was primarily supported by the NSF Hydrologic Sciences Program under Grant No. 1761441 with additional support from the DOE under award DE-SC0019413. Any opinions, findings, and conclusions or recommendations expressed in this material are those of the author(s) and do not necessarily reflect the views of the NSF. Logistical support was facilitated by the DOE WFSFA, the Rocky Mountain Biological Laboratory, and the USDA Forest Service. We thank and acknowledge Jennifer Reithel, Jeffrey Deems, Rosemary Carroll, and Kenneth Williams for assistance in identifying and maintaining field sites. We acknowledge the WY 2019–2021 field observers at Snodgrass: E. Smyth, A. Michell, V. Foley, J. Kaschinske, E. Cruise, L. Coe, E. Hebel, E. Ruggles, A. Koshkin, B. Pritchett, and I. Havlick.

References

Bavay, M., & Egger, T. (2014). MeteoIO 2.4.2: A preprocessing library for meteorological data. *Geoscientific Model Development*, *7*(6), 3135–3151. https://doi.org/10.5194/gmd-7-3135-2014

Bonner, H. M., Raleigh, M. S., & Small, E. E. (2022). Isolating forest process effects on modelled snowpack density and snow water equivalent. *Hydrological Processes*, *36*(1), e14475. https://doi.org/10.1002/hyp.14475

Bonner, H. M., Smyth, E., Raleigh, M. S., & Small, E. E. (2022). A meteorology and snow dataset from adjacent forested and meadow sites at Crested Butte [Dataset]. Zenodo, *1*(3). https://doi.org/10.5281/zenodo.6618553

Brun, E., Martin, E., Simon, V., Gendre, C., & Coleou, C. (1989). An energy and mass model of snow cover suitable for operational avalanche forecasting. *Journal of Glaciology*, *35*(121), 333–342. https://doi.org/10.3189/S0022143000009254

Conway, J. P., Pomeroy, J. W., Helgason, W. D., & Kinar, N. J. (2018). Challenges in modeling turbulent heat fluxes to snowpacks in forest clearings. *Journal of Hydrometeorology*, *19*(10), 1599–1616. https://doi.org/10.1175/JHM-D-18-0050.1

Crawford, J. L., Mcnulty, S. P., Sowell, J. B., & Morgan, M. D. (1998). Changes in aspen communities over 30 years in Gunnison County, Colorado. *The American Midland Naturalist*, *140*(2), 197–205. https://doi.org/10.1674/0003-0031(1998)140[0197:ciacoy]2.0.co;2

Domine, F., Picard, G., Morin, S., Barrere, M., Madore, J.-B., & Langlois, A. (2019). Major Issues in simulating some Arctic snowpack properties using Current detailed snow physics models: Consequences for the thermal regime and water budget of permafrost. *Journal of Advances in Modeling Earth Systems*, *11*(1), 34–44. https://doi.org/10.1029/2018MS001445

Elder, K., Brucker, L., Hiemstra, C., & Marshall, H. (2018). *SnowEx17 community snow pit measurements, version 1*. NASA National Snow and Ice Data Center Distributed Active Archive Center.

Essery, R. (2015). A factorial snowpack model (FSM 1.0). *Geoscientific Model Development*, *8*(12), 6583–6609. https://doi.org/10.5194/gmd-8-3867-2015

Essery, R., Rutter, N., Pomeroy, J., Baxter, R., Stähli, M., Gustafsson, D., et al. (2009). SNOWMIP2: An evaluation of forest snow process simulations. *Bulletin of the American Meteorological Society*, *90*(8), 1120–1136. https://doi.org/10.1175/2009BAMS2629.1

Fang, X., Pomeroy, J. W., DeBeer, C. M., Harder, P., & Siemens, E. (2019). Hydrometeorological data from Marmot Creek research basin, Canadian Rockies. *Earth Systems Science Data*, *11*(2), 455–471. https://doi.org/10.5194/essd-11-455-2019

Hedstrom, N. R., & Pomeroy, J. W. (1998). Measurements and modelling of snow interception in the boreal forest. *Hydrological Processes*, *12*(10–11), 1611–1625. https://doi.org/10.1002/(SICI)1099-1085(199808/09)12:10/11%3C1611::AID-HYP684%3E3.0

Henn, B., Raleigh, M. S., Fisher, A., & Lundquist, J. D. (2013). A comparison of methods for filling gaps in hourly near-surface air temperature data. *Journal of Hydrometeorology*, *14*(3), 929–945. https://doi.org/10.1175/JHM-D-12-027.1

Kakalia, Z., Varadharajan, C., Alper, E., Brodie, E. L., Burrus, M., Carroll, R. W. H., et al. (2021). The Colorado East River community observatory data collection. *Hydrological Processes*, *35*(6), e14243. https://doi.org/10.1002/hyp.14243

Kochendorfer, J., Rasmussen, R., Wolff, M., Baker, B., Hall, M. E., Meyers, T., et al. (2017). The quantification and correction of wind-induced precipitation measurement errors. *Hydrology and Earth System Sciences*, *21*(4), 1973–1989. https://doi.org/10.5194/hess-21-1973-2017

Landry, C. C., Buck, K. A., Raleigh, M. S., & Clark, M. P. (2014). Mountain system monitoring at senator Beck basin, san Juan Mountains, Colorado: A new integrative data source to develop and evaluate models of snow and hydrologic processes. *Water Resources Research*, *50*(2), 1773–1788. https://doi.org/10.1002/2013WR013711

Lehning, M., Fierz, C., & Lundy, C. (2001). An objective snow profile comparison method and its application to SNOWPACK. *Cold Regions Science and Technology*, *33*(2–3), 253–261. https://doi.org/10.1016/S0165-232X(01)00044-1

Lejeune, Y., Dumont, M., Panel, J.-M., Lafaysse, M., Lapalus, P., Le Gac, E., et al. (2019). 57 years (1960–2017) of snow and meteorological observations from a mid-altitude mountain site (Col de Porte, France, 1325 m of altitude). *Earth Systems Science Data*, *11*(1), 71–88. https://doi.org/10.5194/essd-11-71-2019

Liston, G. E., & Elder, K. (2006). A meteorological distribution system for high-resolution terrestrial modeling (MicroMet). *Journal of Hydrometeorology*, *7*(2), 217–234. https://doi.org/10.1175/JHM486.1

Lundquist, J. D., Dickerson-Lange, S., Gutmann, E., Jonas, T., Lumbrazo, C., & Reynolds, D. (2021). Snow interception modeling: Isolated observations have led to many land surface models lacking appropriate temperature sensitivities. *Hydrological Processes*, *35*(7). https://doi.org/10.1002/hyp.14274

Lundquist, J. D., Dickerson-Lange, S. E., Lutz, J. A., & Cristea, N. C. (2013). Lower forest density enhances snow retention in regions with warmer winters: A global framework developed from plot-scale observations and modeling. *Water Resources Research*, *49*(10), 6356–6370. https://doi.org/10.1002/wrcr.20504

Malle, J., Rutter, N., Mazzotti, G., & Jonas, T. (2019). Shading by trees and fractional snow cover control the subcanopy radiation budget. *Journal of Geophysical Research: Atmospheres*, *124*(6), 3195–3207. https://doi.org/10.1029/2018JD029908

Mazzotti, G., Essery, R., Moeser, C. D., & Jonas, T. (2020). Resolving small-scale forest snow patterns using an energy balance snow model with a one-layer canopy. *Water Resources Research*, *56*(1), e2019WR026129. https://doi.org/10.1029/2019WR026129

Mazzotti, G., Essery, R., Webster, C., Malle, J., & Jonas, T. (2020). Process-level evaluation of a hyper-resolution forest snow model using distributed Multisensor observations. *Water Resources Research*, *56*(9), e2020WR027572. https://doi.org/10.1029/2020WR027572

Meek, D. W., & Hatfield, J. L. (1994). Data quality checking for single station meteorological databases. *Agricultural and Forest Meteorology*, *69*(1–2), 85–109. https://doi.org/10.1016/0168-1923(94)90083-3

Ménard, C. B., Essery, R., Barr, A., Bartlett, P., Derry, J., Dumont, M., et al. (2019). Meteorological and evaluation datasets for snow modelling at 10 reference sites: Description of in situ and bias-corrected reanalysis data. *Earth Systems Science Data*, *11*(2), 865–880. https://doi.org/10.5194/essd-11-865-2019

Moeser, D., Mazzotti, G., Helbig, N., & Jonas, T. (2016). Representing spatial variability of forest snow: Implementation of a new interception model. *Water Resources Research*, *52*(2), 1208–1226. https://doi.org/10.1002/2015WR017961

Musselman, K. N., Molotch, N. P., & Brooks, P. D. (2008). Effects of vegetation on snow accumulation and ablation in a mid-latitude sub-alpine forest. *Hydrological Processes*, *22*(15), 2267–2276. https://doi.org/10.1002/hyp.7050

Musselman, K. N., & Pomeroy, J. W. (2017). Estimation of Needleleaf canopy and trunk temperatures and longwave Contribution to melting snow. *Journal of Hydrometeorology*, *18*(2), 555–572. https://doi.org/10.1175/JHM-D-16-0111.1

Musselman, K. N., Pomeroy, J. W., & Link, T. E. (2015). Variability in shortwave irradiance caused by forest gaps: Measurements, modelling, and implications for snow energetics. *Agricultural and Forest Meteorology*, *207*, 69–82. https://doi.org/10.1016/j.agrformet.2015.03.014

Raleigh, M. S., Gutmann, E. D., Van Stan, J. T., Burns, S. P., Blanken, P. D., & Small, E. E. (2022). Challenges and Capabilities in estimating snow mass intercepted in conifer Canopies with tree sway monitoring. *Water Resources Research*, *58*(3). https://doi.org/10.1029/2021WR030972

Rasmussen, R., Baker, B., Kochendorfer, J., Meyers, T., Landolt, S., Fischer, A. P., et al. (2012). How well are we measuring snow: The NOAA/FAA/NCAR winter precipitation test bed. *Bulletin of the American Meteorology Society*, *93*(6), 811–829. https://doi.org/10.1175/BAMS-D-11-00052.1

Reba, M. L., Marks, D., Seyfried, M., Winstral, A., Kumar, M., & Flerchinger, G. (2011). A long-term dataset for hydrologic modeling in a snow-dominated mountain catchment. *Water Resources Research*, *47*(7), W07702. https://doi.org/10.1029/2010WR010030

Roth, T. R., & Nolin, A. W. (2017). Forest impacts on snow accumulation and ablation across an elevation gradient in a temperate montane environment. *Hydrology and Earth System Sciences*, *21*(11), 5427–5442. https://doi.org/10.5194/hess-21-5427-2017

Rutter, N., Essery, R., Pomeroy, J., Altimir, N., Andreadis, K., Baker, I., et al. (2009). Evaluation of forest snow processes models (SnowMIP2). *Journal of Geophysical Research*, *114*(D6), D06111. https://doi.org/10.1029/2008JD011063

Sivy, K. J., Nolin, A. W., Cosgrove, C. L., & Prughm, L. R. (2018). Critical snow density threshold for Dall's sheep (Ovis Dalli Dalli). *Canadian Journal of Zoology*, *96*(10), 1170–1177. https://doi.org/10.1139/cjz-2017-0259

Smyth, E. J., Raleigh, M. S., & Small, E. S. (2020). Improving SWE estimation with data assimilation: The influence of snow depth observation timing and uncertainty. *Water Resources Research*, *56*(5), e2019WR026853. https://doi.org/10.1029/2019WR026853

Storck, P., Lettenmaier, D. P., & Bolton, S. M. (2002). Measurement of snow interception and canopy effects on snow accumulation and melt in a mountainous maritime climate, Oregon, United States. *Water Resources Research*, *38*(11), 515–516. https://doi.org/10.1029/2002WR001281

Strasser, U., Warscher, M., & Liston, G. E. (2011). Modeling snow-canopy processes on an Idealized mountain. *Journal of Hydrometeorology*, *12*(4), 663–677. https://doi.org/10.1175/2011JHM1344.1

Teich, M., Giunta, A. D., Hagenmuller, P., Bebi, P., Schneebeli, M., & Jenkins, M. J. (2019). Effects of bark beetle attacks on forest snowpack and avalanche formation—Implications for protection forest management. *Forest Ecology and Management*, *438*, 186–203. https://doi.org/10.1016/j.foreco.2019.01.052

Trujillo, E., & Molotch, N. P. (2014). Snowpack regimes of the Western United States. *Water Resources Research*, *50*(7), 5611–5623. https://doi.org/10.1002/2013WR014753

Varhola, A., Coops, N. C., Weiler, M., & Moore, R. D. (2010). Forest canopy effects on snow accumulation and ablation: An integrative review of empirical results. *Journal of Hydrology*, *392*(3–4), 219–233. https://doi.org/10.1016/j.jhydrol.2010.08.009

Venäläinen, P., Luojus, K., Lemmetyinen, J., Pulliainen, J., Moisander, M., & Takala, M. (2021). Impact of dynamic snow density on GlobSnow snow water equivalent retrieval accuracy. *The Cryosphere*, *15*(6), 2969–2981. https://doi.org/10.5194/tc-15-2969-2021

Wayand, N. E., Massamann, A., Butler, C., Keenan, E., Stimberis, J., & Lundquist, J. D. (2015). *A meteorological and snow observational data set from snoqualmie pass (921 m)*. U.S. University of Washington ResearchWorks Archive. Retrieved from http://hdl.handle.net/1773/25611